

# Experimental Investigation of Isochoric and Isobaric Compressed Air Energy Storage Systems for Power Generation

Mebratu Adamu Assegie<sup>1</sup> , Pankaj Kalita<sup>1\*</sup> , Niranjana Sahoo<sup>2</sup> , Pushpendra Singh<sup>1</sup> 

<sup>1</sup> School of Energy Science and Engineering, Indian Institute of Technology Guwahati, Guwahati 781039, Assam, India

<sup>2</sup> Department of Mechanical Engineering, Indian Institute of Technology Guwahati, Guwahati 781039, Assam, India

\* Correspondence author: [pankajk@iitg.ac.in](mailto:pankajk@iitg.ac.in)

Scopus Author ID [8263464800](#)

Received: 10 December 2024; Accepted: 25 December 2024; Published: 21 January 2025

**Abstract:** Compressed Air Energy Storage (CAES) is a promising energy storage solution that enhances renewable energy efficiency while being cost-effective and environmentally sustainable. This study experimentally compared isobaric and isochoric CAES systems for power generation at a storage pressure of 6 bar, focusing on their charging, discharging, and overall electrical efficiency. During the charging phase, isobaric systems stored 1.54 kWh of more energy than the isochoric system. The maximum compressor outlet temperatures of isobaric and isochoric systems are found to be 91.2 °C and 120.5 °C respectively. The discharging phase revealed significant performance differences: the isochoric system achieved a maximum airflow rate of 72.92 m<sup>3</sup>/h and rotational speed of 1191 RPM, compared to the isobaric system's 48.6 m<sup>3</sup>/h and 1098 RPM. However, the isochoric system discharged its energy in 130 seconds, while the isobaric system sustained discharge for 195 seconds. Electrical efficiency was 62.82% higher for the isobaric system than for the isochoric system. This study highlights the operational advantages and limitations of each system, providing valuable insights for optimizing CAES technologies.

**Keywords:** Energy storage; Isobaric and Isochoric storage tank; power generation, Efficiency

## 1. Introduction

Electricity is distinctive in that it must be consumed the moment it is generated. To maintain a consistent and efficient power flow from generation to end users, the transmission system must balance supply and demand continuously, particularly during peak usage periods. Any mismatch between these can lead to disruptions in the power system's stability and quality. This challenge is especially significant for intermittent energy sources such as wind and solar, where fluctuations in output can occur. Energy storage systems (ESS) are vital in addressing this issue by providing a real-time balance between production and consumption. ESS enhances grid management and reliability, allowing renewable energy sources to integrate more effectively into the power system. Furthermore, they improve energy quality by stabilizing grid frequency and voltage, thereby enabling a higher penetration of renewables and ensuring a more resilient energy supply [1]. Therefore, based on its application for large-scale energy storage, its capital cost is comparable in the faces of other energy storage technologies, relatively small self-discharge ratio, longer lifetime, and life cycle. A compressed air energy storage system is selected for further research work [2].

Compressed air energy storage is one of the most promising large-scale energy storage schemes that should be used in the power system. The first commercial CAES power plant was developed at Huntorf, Germany, in 1978 with a capacity of 290MW, and McIntosh in the US in 1991 installed a capacity of 110 MW. The purpose of this power plant was to store excess energy that was generated during night-time when energy demand was low [3].

Energy and thermodynamics were examined in an innovative micro compressed air energy storage system (micro-CAES). The charge phase utilized 534 kWh, mostly renewable. Discharge produced 281 kWh at 52% round-trip efficiency. There were 189 kWh of thermal storage during compression and 139 kWh of refrigeration energy during expansion [4]. Analyzing a constant-pressure air storage system utilizing compressed gas energy and nonlinear cam dynamics. The new isobaric compressed air storage device improves constant pressure and energy efficiency. A 0.4MPa pneumatic system saves 18% energy while maintaining 2.14% compressed air pressure [5]. Isobaric storage systems were limited by their complexity, cost, and by the fact that the water pumps required to maintain a constant air pressure consume 15% of the generated electricity. Micro-compressed air energy storage operating on an isobaric system maintained with a water column was studied for its energy and exergy efficiency. The study showed that the micro-CAES system is highly effective in distributed power networks. Further, its flexibility allows the small-scale CAES system with a quasi-isothermal compression and expansion process to provide an effective and good system efficiency [6].

The integrated I-CAES system with pumped hydro storage integrated design demonstrates that the power produced and consumed in the I-CAES system was constant, while the power consumed and produced in the hydraulic portion was 37% and 23% of the total power, respectively. Furthermore, the exergy stored in large caverns decreased by 3.6% and 8.4% for 100 m and 200 m deep water heights, respectively [7]. Analysis of an innovative small-scale spring-actuated scissor-jack installed constant pressure CAES reservoir design analysis was carried out. The tank under consideration was subjected to both theoretical design and structural examination. In light of this, one may draw the conclusion that the effectiveness of the air energy storage reservoir was observed to be 95% accuracy [8]. A novel combined pumped hydro and compressed air energy storage (PH-CAES) system performances were experimentally studied, focusing on power generation systems. The result revealed that the power conversion efficiency and the exergy efficiency were 45% and 30% respectively [9]. The multi-level underwater compressed air energy storage (UWCAES) system performance was investigated based on thermodynamic modeling and analysis. The result presents that the exergy efficiency of the multi-level UWCAES system was found to be between 62% and 82% without and with integrated battery packs, respectively [10].

Compressed air energy storage systems can be classified into constant volume and constant pressure systems based on storage mechanisms. The literature survey highlights that Compressed Air Energy Storage (CAES) is a promising technology for energy storage and recovery. This innovative approach can significantly enhance the efficiency of renewable energy systems while maintaining cost-effectiveness. CAES provides an environmentally sustainable solution by reducing reliance on fossil fuels and offers operational flexibility, making it well-suited for integrating intermittent renewable energy sources into the power grid.

Despite its potential, several challenges persist, particularly in the design and operational efficiency of storage systems.

Conventional CAES systems predominantly employ **isochoric (constant volume)** air storage tanks. While widely used, this approach suffers from several drawbacks that limit its overall efficiency. During the discharging phase, the air storage pressure decreases as compressed air is released to the expander for power generation. This pressure drop reduces the expander's performance, which operates under varying pressure ratios, ultimately leading to a decline in system efficiency. On the other hand, **isobaric (constant pressure)** CAES systems, which are still in the research and development stage, offer a promising alternative by maintaining a nearly constant pressure during both charging and discharging. This is achieved by allowing the storage volume to vary dynamically. By avoiding pressure fluctuations, isobaric systems ensure that the expander operates under a steady pressure ratio, which enhances overall efficiency and simplifies system operation. However, the development and implementation of isobaric systems require innovative engineering solutions to design storage tanks capable of withstanding variable volume changes while maintaining operational reliability and safety.

This study is an entirely experimental investigation into the performance of isochoric and isobaric CAES systems, with a focus on power generation applications. For the isochoric system, a repurposed air storage tank, originally part of an ELGI two-stage reciprocating compressor setup, was utilized. In contrast, the isobaric storage system was custom-designed and fabricated specifically for this research. The isobaric tank features an advanced mechanism that integrates a spring-actuated scissor jack with a piston assembly, enabling controlled volume adjustments to maintain constant pressure during operation. This innovative design addresses the limitations of isochoric systems and provides practical insights into the feasibility and efficiency of isobaric systems under experimental conditions.

By experimentally comparing these two CAES configurations, this study provides valuable contributions to the understanding of their operational performance. It offers a practical evaluation of the potential benefits and challenges associated with isobaric systems while highlighting their ability to overcome the efficiency limitations inherent in isochoric systems. The findings aim to advance the development of CAES technologies and promote their practical adoption in renewable energy applications.

## 2. Experimental Methodology

The experimental test was performed using the same size, small-scale isochoric and isobaric storage tanks. The key elements of the experimental arrangement comprise a two-stage oil-lubricated reciprocating ELGi Compressor Model TS 303, which is crucial for compressing air. The system also features an air receiver with a capacity of 220 litres, which stores the compressed air.

The isobaric CAES system storage tank, used to perform various experimental works, features a spring-actuated scissor-jack assembled tank with a capacity of 220 liters and has been utilized alongside essential safety valves. Additionally, a vane air turbine is coupled with an alternator to convert the stored energy into electrical power. The setup is further equipped with a load bank to simulate varying loads and assess system performance under different conditions. Various measuring instruments are employed, including temperature sensors,

pressure transmitters, pressure gauges, energy meters, and RPM meters/counters, to monitor and record operational data. These instruments are connected to a data logging system with a processing unit, as schematically depicted in Figure 1, which enables detailed data collection and analysis throughout the experimental process.

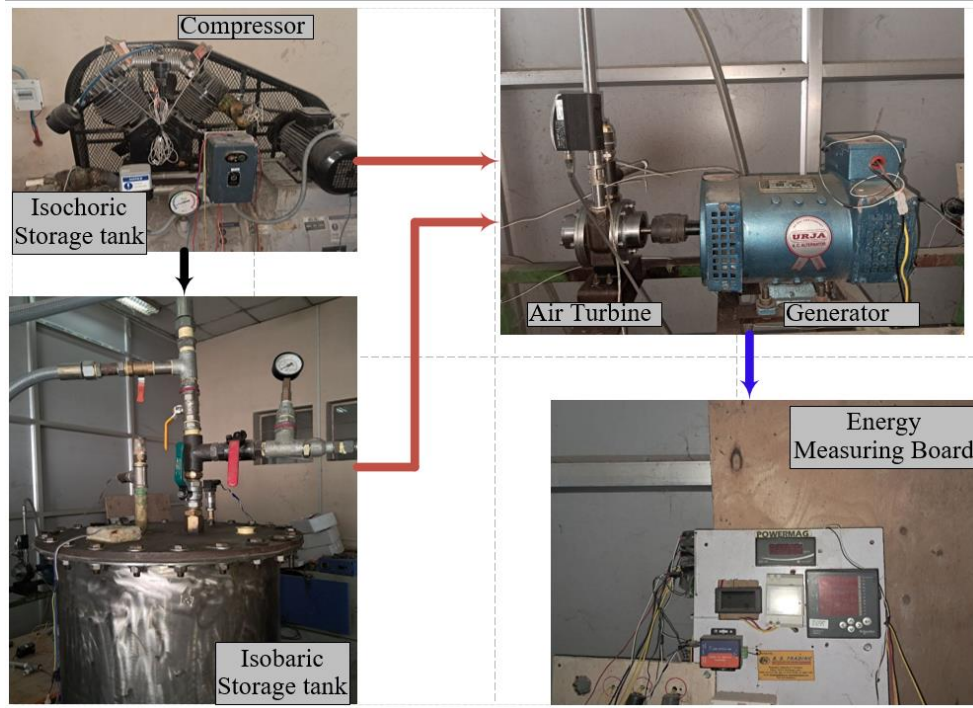


**Figure 1.** Simple Experimental Setup

### 3. Formulation of Compression and Expansion

This section may be divided by subheadings. It should provide a concise and precise description of the experimental results, their interpretation as well as the experimental conclusions that can be drawn.

#### 3.1. Compression Process

The compression process was performed using a two-stage reciprocating compressor. The total energy spent is the combined energy consumed by the low-pressure compressor and the high-pressure compressor and is defined as: [12].

The compression process was performed using a two-stage reciprocating compressor. The total energy spent is the combined energy consumed by the low-pressure compressor and the high-pressure compressor and is defined as: [12].

The low-pressure compressor energy consumption is calculated from Eq. (1):

$$W_{LPC} = \frac{1}{\eta_c} \frac{k}{k-1} R \dot{m} T_{in,LPC} \left[ \left( \frac{P_{out,LPC}}{P_{in,LPC}} \right)^{\frac{k-1}{k}} - 1 \right] \quad (1)$$

where,  $T_{in,LPC} = 303.15\text{ K}$  represents the intake air temperature for the low-pressure compressor, which is assumed to be the same as the ambient temperature.  $\eta_c = 0.843$ , refers to the efficiency of the compressor.  $k = 1.4$ , represents the adiabatic index.  $R = 8.314\text{ J / mol} \cdot \text{K}$ , refers to the gas constant.  $\dot{m}$ , represents the mass flow rate of air.  $P_{in,LPC} = 101.325\text{ kPa}$ , refers to the pressure at the intake of the low-pressure compressor, which is typically assumed to be equal to the ambient pressure.  $P_{out,LPC}$ , represents the outlet pressure of the low-pressure compressor, which is defined as an intermediate pressure between the two compressors. Hence, the output temperature of the low-pressure compressor ( $T_{HPC,out}$ ) can also be determined from Eq. (2) [13]:

$$T_{LPC,out} = T_{HPC,in} \left( \frac{P_{LPC,out}}{P_{LPC,in}} \right)^{\frac{n-1}{n}} \quad (2)$$

The intermediate pressure between the low-pressure compressor and high-pressure compressor is calculated from Eq. (3) [14].

$$P_{out,LPC} = \sqrt{P_{in,LPC} \times P_{out,HPC}} \quad (3)$$

The low-pressure compressor energy consumption is calculated from Eq. (4):

$$W_{HPC} = \frac{1}{\eta_c} \frac{k}{k-1} R \dot{m} T_{in,HPC} \left[ \left( \frac{P_{out,HPC}}{P_{in,HPC}} \right)^{\frac{k-1}{k}} - 1 \right] \quad (4)$$

where,  $T_{in,HPC}$  represents the inlet temperature of the high-pressure compressor, which is assumed to be the same as the  $T_{in,LPC}$  due to perfect inter-cooling assumption.  $\eta_c$  refers to the efficiency of the compressor.  $k$ , represents the adiabatic index.  $R$  refers to the gas constant.  $\dot{m}$ , represents the mass flow rate of air.  $P_{in,HPC}$ , refers to the inlet pressure of the high-pressure compressor, which is typically assumed to be equal to the intermediate pressure  $P_{out,LPC}$  or the outlet pressure of the low-pressure compressor. Whereas  $P_{out,HPC}$ , represents the outlet pressure of the high-pressure compressor, which is the designed or pre-determined pressure of the high-pressure compressors specifically case study: 6 bar. Hence, the total amount of compressor-consumed energy (input electrical energy,  $W_c$ ) could be calculated as follows in Eq. (5),

$$W_c = \sum_1^2 W_{c,N} = W_{LPC} + W_{HPC} \quad (5)$$

### 3.2. Expansion Process

The expansion process for both the isobaric and isochoric storage tanks was performed using a DAM-6 AM-2 model vane motor/turbine. Hence, the total amount of the generated energy (output electrical energy,  $W_e$ ) during the discharge process is calculated by Eq. (6) [12]:

$$W_e = \int_0^m \eta_e \eta_g \frac{k}{k-1} R \dot{m} T_{e,M}^{in} \left[ 1 - \left( \frac{P_{e,m}^{in}}{P_{e,m}^{out}} \right)^{\frac{k-1}{k}} \right] dt \quad (6)$$

For single-stage Expansion, the output electrical energy is determined using Eq. (7):

$$W_e = \eta_e \eta_g \frac{k}{k-1} R \dot{m} T_e^{in} \left[ 1 - \left( \frac{P_e^{in}}{P_e^{out}} \right)^{\frac{k-1}{k}} \right] \quad (7)$$

where,  $T_{e,M}^{in}$  refers to the inlet air temperature of the M-stage expansion,  $\eta_e$  is the adiabatic efficiency of expansion,  $\eta_g$  is generator efficiency,  $P_{e,m}^{in}$  and  $P_{e,m}^{out}$  are inlet and outlet pressures of M-stage expansion, respectively.

#### 4. Results and Discussion

An experimental study was conducted on both isobaric and isochoric compressed air energy storage (CAES) systems to assess their performance and efficiency under controlled conditions. The experiments were designed to evaluate the energy usage during the charging process and the amount of energy retained within the system, and the energy output during discharging, all while maintaining a constant pressure of 6 bar. Key parameters measured included the average electrical power consumed by the compressor during charging, the power generated during discharging, and the respective durations for both the charging and discharging phases.

In the charging phase, a comprehensive examination of storage conditions was performed, particularly observing variations in pressure and temperature within the storage tanks. This detailed analysis helped in understanding; how these factors influence energy retention in each system type. Similarly, during the discharging phase, the study focused on monitoring electrical parameters, including voltage, current, power output, and the rotational speed (RPM) of the generator. These metrics provided insights into how effectively each system could convert stored air energy back into electrical energy.

Finally, the electrical efficiency of the isobaric and isochoric storage tanks was compared, taking into account the energy balance between input during charging and output during discharging. This comparative analysis aims to identify the advantages and limitations of each storage type, providing valuable insights into their potential applications and overall suitability for CAES operations at a set pressure of 6 bar.

##### 4.1. Charging Process

The basic storage parameters that are discussed during the compression process for both isobaric and isochoric storage tanks were the power consumption, the temperature generation, and the pressure for the test condition of 6-bar pressure. The charging process experiment was performed with an ambient temperature of 30 °C and a relative humidity of 65%. The outlet pressure and temperature of the air storage tank are obtained based on the pressure gauges attached to the isochoric storage tank and pressure sensors installed on the top of isobaric

energy storage reservoir. Whereas the intermediate pressure is calculated from the experimental results and Eq. (3).

The time taken and the energy stored at 6 bar pressure for both the isochoric and isobaric storage tanks were 0.104 and 8.49 kWh, and 0.123 and 10.03 kWh respectively. The compression process temperatures were recorded by thermocouples installed in each section of the device. The low-pressure compressor has an intake temperature of 30°C, which is the ambient temperature. The maximum experimental outlet temperatures of the low-pressure compressor recorded for 6-bar pressure was 91.171°C (364.321 K). Whereas, the maximum experimental outlet temperature of the second stage compressor was recorded as 120.495°C (393.645 K). On the other hand, the numerical evaluation of temperature for both the low and high-pressure compressor considering heat transfer through packed bed thermal energy system calculated by Eq. (2) was 376.60 K and 393.57 K, respectively, which is approximately the same as the experimentally obtained. The pressure conditions recorded using the obtained were inlet pressure 1.01325 bar, intermediate pressure 2.387 bar, and 5.98 bar whereas the numerically computed pressure was only considered the intermediate pressure computation because the remaining pressures were the ambient pressure 1.0325 bar and the designed pressure 6 bar and as it is observed the pressures were approximately similar with the experimentally obtained pressures.

#### *4.2. Discharging Process*

The discharge process of the isobaric and isochoric CAES tanks was studied at 6 bar pressure. The study focused on analyzing the storage pressure (Pa), voltage output (V), current output (I), power output (W), turbine generator coupling rotating speed (RPM), and compressed air flow/consumption (m<sup>3</sup>/h.) required to operate the turbine. The discharging experiment for the isobaric CAES tank considers the leakage pressure during its storage duration due to it being manufactured and built in the institute, and it is under investigation. However, the isochoric storage tank is factory-manufactured, and its leakage is considered negligible.

#### *4.3. Pressure Profile*

The isobaric storage tank's average pressure was recorded as 5.98 bar during its storage period, and it also experienced 1.39 bar pressure leakage, whereas the isochoric storage pressure remained at 6 bar pressure during its storage period. The pressure profile for both the isobaric and isochoric storage tanks is shown in Figure 2.

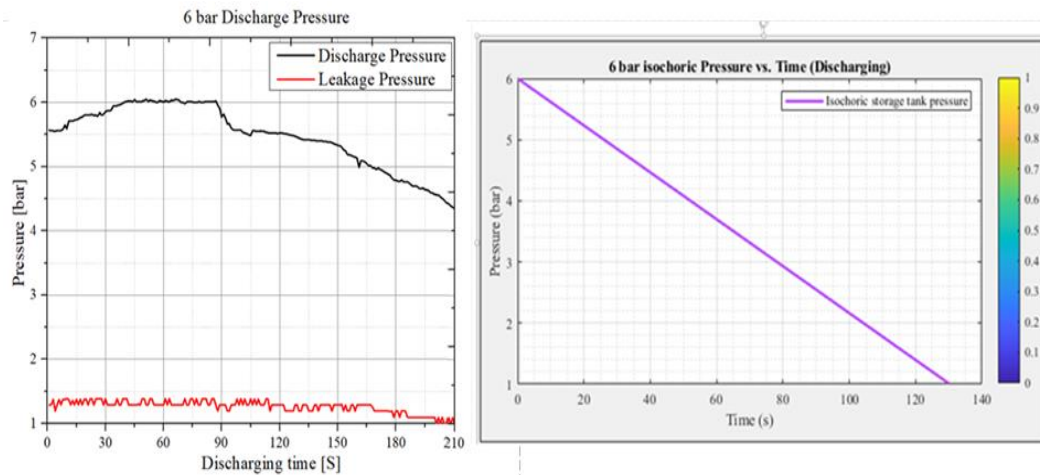


**Figure 2.** Pressure profile for isobaric and isochoric storage tanks during discharging time

#### 4.4. Compressed Air Flow and RPM Profile

The amount of compressed air used for power generation in isobaric and isochoric storage tanks for the 6-bar pressure conditions, is shown in Figure 3 and Figure 4. The red line depicts the isochoric test results whereas the black line shows the isobaric test results. Whereas the discharging time of the isochoric and isobaric storage tanks at pressure of 6 bar, were recorded as 130 seconds (0.0361 hours) and 195 seconds (0.0542 hours) respectively. As shown in Figure 3 the highest flow rate recorded for the isochoric storage flow rate reached 72.92 m<sup>3</sup>/h., and the isobaric flow rate was 48.6 m<sup>3</sup>/h. On the other hand, the rotational speed of the turbine and generator system during power generation in isobaric and isochoric storage tanks is illustrated in Figure 4. The maximum rotational speeds of the turbine and generator system were recorded for isochoric pressure was 1191 RPM, and for isobaric pressure, it was 1098 RPM.

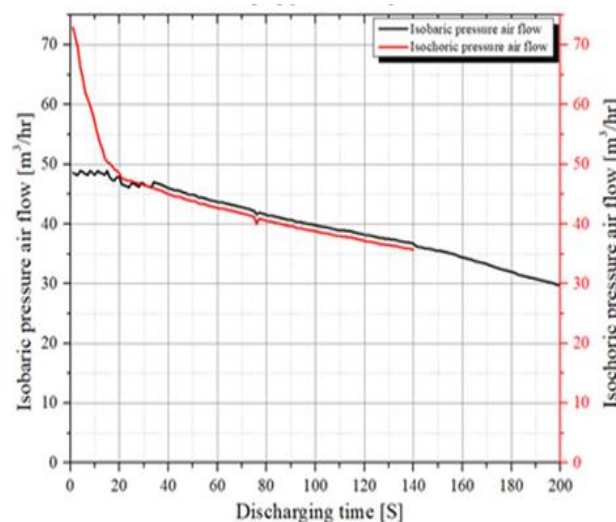


**Figure 3.** Outlet air pressure from isochoric and isobaric storage tank during discharging



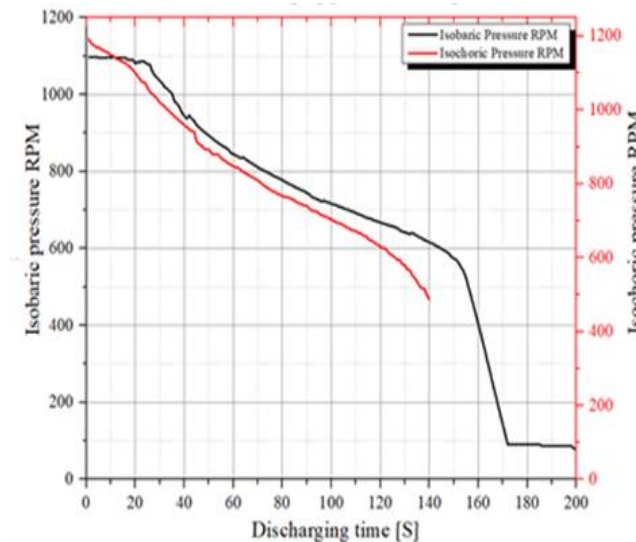


**Figure 4.** RPM profile for isochoric and isobaric storage tank during discharging

#### 4.5. Electrical Voltage and Current Output Profile

The voltage (V) and Current (I) output of the generator system during the expansion period in the isobaric and isochoric storage tanks for the 6 bar pressure is illustrated in Figure 5 and Figure 6. The red line graph reflects the findings of the isochoric test, while the black line depicts the results of the isobaric test, to clearly illustrate the variances. Whereas the discharging time of the isochoric and isobaric storage tanks at pressure of 6 bar, were recorded as 130 seconds (0.0361 hours) and 195 seconds (0.0542 hours) respectively. Hence, as shown in Figure 5 the maximum Voltage recorded at 6 bar pressure was 213.6 Volts under constant volume conditions and 186.9 Volts under constant pressure conditions. On the other hand, Figure 6 illustrates the maximum current was recorded to be 0.63 Amperes for isochoric pressure and 0.67 Amperes for isobaric pressure at 6 bar.

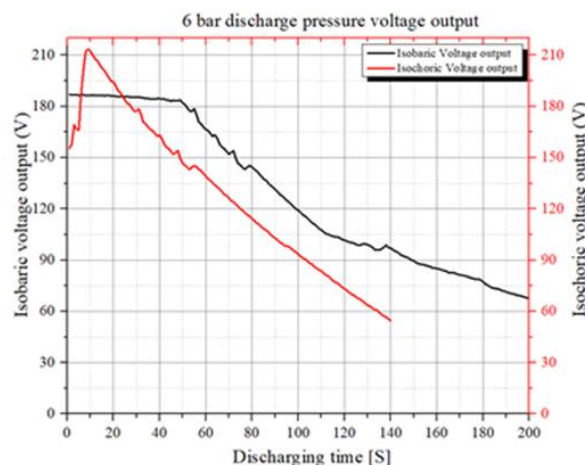


**Figure 5.** Output Voltage for isochoric and isobaric storage tank during discharging time

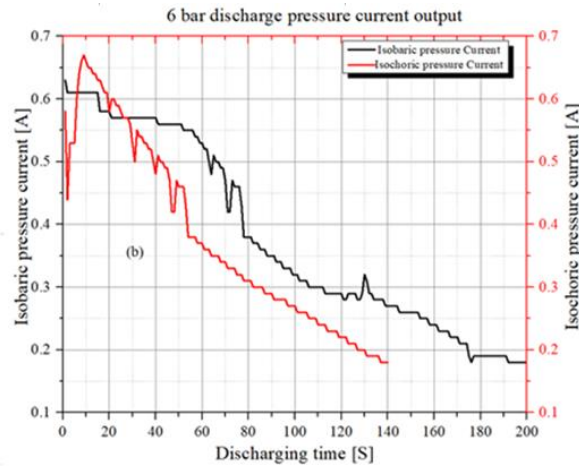


**Figure 6.** Output current for isochoric and isobaric storage tank during discharging time

#### 4.6. Electrical Power Output

The power production of the generator system during the expansion period in the isobaric and isochoric storage tanks under 6 bar pressure conditions, is denoted in Figure 7.

The red line graph reflects the isochoric test findings, while the black line indicates the isobaric test results. Whereas the discharging time of the isochoric and isobaric storage tanks at pressure of 6-bar, were recorded as 130 seconds (0.0361 hours) and 195 seconds (0.0542 hours) respectively. Hence, as shown in Figure (7), the highest power output of the generator system recorded at 6 bar pressure was 94.8W for isochoric and 85.95W for isobaric.

#### 4.7. Electrical Efficiency

The electrical efficiency for both the isobaric and isochoric storage tanks is determined by assessing the electrical energy generated by expansion turbines when needed and the electrical energy consumed by the compressors during the charging process. It is defined in Eq. (8) [13,15,16].

$$\eta_{elec} = \frac{E_{elec,T}}{E_{elec,C}} \quad (8)$$

where,  $\eta_{elec}$ : electrical efficiency,  $E_{elec,T}$ : electrical energy output from expansion turbine, and  $E_{elec,C}$ : electrical energy consumed during compression.

The electrical energy stored and generated in both the isobaric and isochoric storage tank experimentally obtained were 1.305 kWh and 0.777 kWh respectively. Moreover, the electrical efficiency for the isochoric storage tank was 7.8%, and, for the isobaric storage tank is obtained as 12.7% at 6 bar pressure.

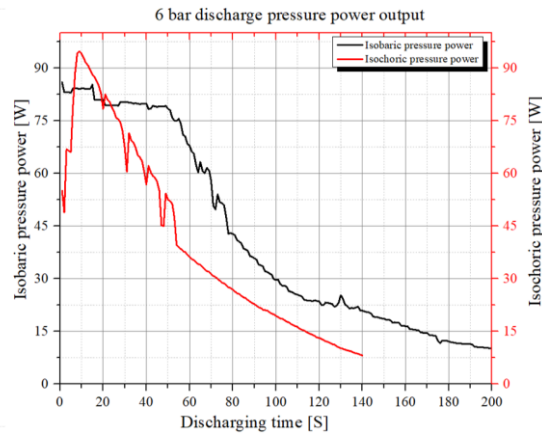


**Figure 7.** Output profile for isochoric and isobaric storage tank during discharging time

#### 4.8. Discussion of Results

The experimental investigation compared the performance of constant volume and constant pressure compressed air energy storage (CAES) systems during power generation. The findings (Figure 2 to Figure 7) illustrate that the isobaric storage tank exhibits a significantly longer operating time compared to the isochoric storage tank. This distinction is evident across various performance parameters, including compressed air flow/consumption ( $\text{m}^3/\text{h.}$ ), turbine generator coupling rotating speed (RPM), voltage output (V), current output (I), and power output (W).

The prolonged operating time of the constant-pressure storage tank is attributed to its ability to maintain a steady pressure during the discharging of compressed air. This is achieved by allowing the storage tank's volume to change dynamically during storage and generation. In this study, a spring-operated scissor-jack assembled piston mechanism was integrated into the isobaric tank design. This innovative mechanism ensures that the internal pressure remains constant while the air volume adjusts as needed. The resulting constant-pressure conditions lead to a more uniform air flow rate, enabling consistent and extended discharge durations.

In contrast, the isochoric storage tank operates with a fixed volume, causing the internal pressure to decrease as air is released. During the initial stages of discharge, the pressure within the isochoric tank is relatively high, resulting in a substantial air flow rate. However, as the discharge progresses, the declining pressure leads to a corresponding reduction in flow rate. Additionally, the pressure drop is accompanied by a significant decrease in air temperature, which further limits the air release rate. Consequently, the energy release period for the isochoric tank is shorter, and the stored air is depleted more rapidly.

From a thermodynamic perspective, the differences between the two storage systems are rooted in the work done during their respective processes. In an isobaric process, the work done by the air can be expressed as  $W = P\Delta V$ , where  $P$  is the constant pressure and  $\Delta V$  is the change in volume. This implies that energy is released gradually and continuously as the volume varies, resulting in an extended period of operation. In contrast, the work done in an isochoric process is zero ( $W = P\Delta V = 0$ , for  $V = \text{constant}$ ). The energy release in an isochoric system is driven solely by changes in internal energy, which occur rapidly at first and diminish as the pressure and temperature decrease.

The experimental results further emphasize the operational efficiency and performance advantages of isobaric storage systems over isochoric systems. By maintaining constant pressure, the isobaric system ensures stable energy output and a more predictable discharge profile. This study's innovative use of a spring-actuated scissor-jack assembled piston mechanism highlights the potential for isobaric systems to overcome the limitations associated with conventional isochoric storage systems, particularly in terms of energy release duration and consistency.

Overall, the findings underscore the significant advantages of isobaric CAES systems for applications requiring sustained and reliable energy output, offering valuable insights for advancing energy storage technologies. This in-house developed isobaric CAES system offers practical applications that set it apart from conventional isobaric configurations. This design functions efficiently without relying on specific geographic features like deep seabed's or depleted salt caverns, nor complex throttling mechanisms to maintain constant pressure. The isobaric system features an innovative spring-operated scissor-jack piston mechanism, which enables controlled volume adjustments, ensuring stable performance throughout the discharge phase. However, assembling and fitting the piston mechanism requires specialized skills, presenting a limitation that could be addressed through improved design or training. In comparison, the isochoric CAES system utilized in this study is a factory-made, conventional compressed air storage tank. While this system exhibited high instantaneous performance metrics, its rapid pressure decline during discharge resulted in a shorter operational duration, limiting its ability to sustain energy release over time. The findings from this study emphasize the adaptability of the novel isobaric CAES system for diverse energy storage scenarios. Future multidisciplinary research could focus on refining the assembly process, incorporating advanced materials, exploring hybrid configurations, and optimizing system designs to enhance efficiency, scalability, and ease of deployment. These advancements would significantly expand the scope and applicability of CAES technologies, addressing the growing demand for sustainable and reliable energy storage solutions across various sectors.

## 5. Conclusions

This study provides a comprehensive experimental comparison of constant-volume and constant-pressure compressed air energy storage (CAES) systems for power generation, focusing on their performance, efficiency, and operational characteristics at a pressure of 6 bar. The findings reveal critical differences between the two systems, offering valuable insights for their optimization and application in renewable energy storage. The **isobaric CAES system** demonstrated superior overall performance, achieving an electrical efficiency of 12.7% compared to 7.8% for the isochoric system. This advantage is primarily attributed to the system's ability to maintain a consistent pressure throughout the discharging process. By ensuring a uniform air flow, the isobaric system achieved an extended discharge duration of 195 seconds, enabling more effective energy recovery. In contrast, the **isochoric CAES system**, characterized by its constant volume design, exhibited higher instantaneous performance metrics. These include a peak airflow rate of 72.92 m<sup>3</sup>/h, a rotational speed of 1191 RPM, and a maximum power output of 94.8 W. These findings underscore the distinct advantages of each system for different applications. The isobaric CAES system is better suited for scenarios requiring consistent and prolonged energy discharge, making it an ideal candidate

for renewable energy integration and grid stability. Although the instantaneous performance metrics for both storage tanks were expected to be the same, the isobaric storage tank exhibited slightly lower performance due to minor leakage. This occurred because the isobaric system was assembled using a bolted design to facilitate maintenance and to verify the functionality of the new piston and scissor-jack mechanism. As this mechanism is novel, the bolted configuration allowed for easier inspection and adjustments. Once the system demonstrates consistent and reliable performance, the final product will be fully welded to eliminate leakage, ensuring it performs at the same pressure as the isochoric storage tank and generates better efficiency than the existing isobaric efficiencies. Conversely, the isochoric system's high initial power output makes it advantageous for applications that demand quick bursts of energy.

## Multidisciplinary Domains

This research primarily focuses on two critical domains: (a) mechanical engineering, and (b) energy storage technologies. It aims to contribute to the advancement of sustainable energy solutions by integrating innovative approaches within these fields.

## Funding

This research received no external funding

## Conflicts of Interest

The authors declare no conflict of interest.

## References

- [1] Ibrahim, H.; Beguenane, R.; Merabet, A. Technical and Financial Benefits of Electrical Energy Storage. In *Proceedings of the 2012 IEEE Electr. Power Energy Conf. (EPEC)*, London, ON, Canada, **2012**; pp. 86–91, <https://doi.org/10.1109/EPEC.2012.6474985>.
- [2] Chen, H.; Cong, T.N.; Yang, W.; Tan, C.; Li, Y.; Ding, Y. Progress in Electrical Energy Storage System: A Critical Review. *Prog. Nat. Sci.* **2009**, *19*, 291–312, <https://doi.org/10.1016/j.pnsc.2008.07.014>.
- [3] Zunft, S.; Jakiel, C.; Koller, M.; Bullough, C. Adiabatic Compressed Air Energy Storage for the Grid Integration of Wind Power. In *Proceedings of the Sixth International Workshop on Large-Scale Integration of Wind Power Transmission Networks Offshore Wind Farms*, Delft, The Netherlands, **2006**; pp. 26–28.
- [4] De Lieto Vollaro, R.; Faga, F.; Tallini, A.; Cedola, L.; Vallati, A. Energy and Thermodynamical Study of a Small Innovative Compressed Air Energy Storage System (Micro-CAES). *Energy Procedia* **2015**, *82*, 645–651, <https://doi.org/10.1016/j.egypro.2015.12.017>.
- [5] Wang, H.; Tong, Z.; Dong, X.; Xiong, W.; Ting, D.S.K.; Cariveau, R.; et al. Design and Energy Saving Analysis of a Novel Isobaric Compressed Air Storage Device in Pneumatic Systems. *J. Energy Storage* **2021**, *38*, 102614, <https://doi.org/10.1016/j.est.2021.102614>.
- [6] Kim, Y.M.; Favrat, D. Energy and Exergy Analysis of a Micro-Compressed Air Energy Storage and Air Cycle Heating and Cooling System. *Energy* **2010**, *35*, 213–220, <https://doi.org/10.1016/j.energy.2009.09.011>.
- [7] Kim, Y.M.; Shin, D.G.; Favrat, D. Operating Characteristics of Constant-Pressure Compressed Air Energy Storage (CAES) System Combined with Pumped Hydro Storage Based on Energy and Exergy Analysis. *Energy* **2011**, *36*, 6220–633, <https://doi.org/10.1016/j.energy.2011.07.040>.
- [8] Assegie, M.A.; Siram, O.; Kalita, P.; Sahoo, N. Novel Small-Scale Spring Actuated Scissor-Jack Assembled Isobaric Compressed Air Energy Storage Tank: Design Analysis and Simulation. *J. Energy Storage* **2024**, *89*, 111627, <https://doi.org/10.1016/j.est.2024.111627>.

- [9] Camargos, T.P.L.; Pottie, D.L.F.; Ferreira, R.A.M.; Maia, T.A.C.; Porto, M.P. Experimental Study of a PH-CAES System: Proof of Concept. *Energy* **2018**, *165*, 630–638, <https://doi.org/10.1016/j.energy.2018.09.109>.
- [10] Wang, Z.; Ting, D.S.K.; Cariveau, R.; Xiong, W.; Wang, Z. Design and Thermodynamic Analysis of a Multi-Level Underwater Compressed Air Energy Storage System. *J. Energy Storage* **2016**, *5*, 203–211, <https://doi.org/10.1016/j.est.2016.01.002>.
- [11] Olabi, A.G.; Wilberforce, T.; Ramadan, M.; Abdelkareem, M.A.; Alami, A.H. Compressed Air Energy Storage Systems: Components and Operating Parameters—A Review. *J. Energy Storage* **2021**, *34*, 102000, <https://doi.org/10.1016/j.est.2020.102000>.
- [12] Cheayb, M.; Marin Gallego, M.; Tazerout, M.; Poncet, S. Modelling and Experimental Validation of a Small-Scale Trigenerative Compressed Air Energy Storage System. *Appl. Energy* **2019**, *239*, 1371–1384, <https://doi.org/10.1016/j.apenergy.2019.01.222>.
- [13] Maia, T.A.C.; Barros, J.E.M.; Cardoso Filho, B.J.; Porto, M.P. Experimental Performance of a Low-Cost Micro-CAES Generation System. *Appl. Energy* **2016**, *182*, 358–364, <https://doi.org/10.1016/j.apenergy.2016.08.120>.
- [14] Lugo-Méndez, H.; Lopez-Arenas, T.; Torres-Aldaco, A.; Torres-González, E.V.; Sales-Cruz, M.; Lugo-Leyte, R. Interstage Pressures of a Multistage Compressor with Intercooling. *Entropy* **2021**, *23*, 351, <https://doi.org/10.3390/e23030351>.
- [15] Elmegaard, B.; Brix, W. Efficiency of Compressed Air Energy Storage. In *Proceedings of the 24th International Conference on Efficiency, Cost, Optimization, Simulation, and Environmental Impact of Energy Systems (ECOS)*, Novi Sad, Serbia, **2011**; pp. 2512–2523.
- [16] Jannelli, E.; Minutillo, M.; Lubrano Lavadera, A.; Falcucci, G. A Small-Scale CAES (Compressed Air Energy Storage) System for Stand-Alone Renewable Energy Power Plant for a Radio Base Station: A Sizing-Design Methodology. *Energy* **2014**, *78*, 313–322, <https://doi.org/10.1016/j.energy.2014.10.016>.